American Journal of Modern Physics
2026, Vol. 15, No. 5, pp. 140–147
https://doi.org/10.11648/j.ajmp.20261505.11

Research Article

Numerical Simulation of the Performance of the Cu(In,Ga)Se_2-based Solar Photovoltaic Cell as a Function of the Space Charge Region Width

Daouda Oubda[1, *], Alfred Bayala[2], Winde Nongue Daniel Koumbem[2], Yacouba Coulibaly[3], Francois Zougmore[1]

[1]Materials and Environment Laboratory, Joseph Ki-Zerbo University, Ouagadougou, Burkina Faso

[2]Thermal and Renewable Energy Laboratory, Joseph Ki-Zerbo University, Ouagadougou, Burkina Faso

[3]Laboratory of Materials, Heliophysics and Environment, Nazi Boni University, Bobo-Dioulasso, Burkina Faso

Abstract

In a global context marked by constantly increasing energy demand, dwindling fossil fuel resources, and growing environmental concerns, the search for alternative, clean, and sustainable energy sources has become essential. Several questions remain regarding the production of abundant, low-cost energy without environmental impact. Therefore, optimizing the performance of thin-film photovoltaic (PV) solar cells has been the subject of numerous studies. Our study falls within this perspective and analyzes the role of the space charge region (SCR) in the performance optimization process. The aim of our study is to obtain improved electrical parameters. To achieve this objective, we opted for numerical simulation with One-dimensional Solar Cell Capacities Simulation software (SCAPS-1D) of the Mo/CIGS/CdS/ZnO structure. The results obtained show a significant decrease in the open circuit voltage (V_{OC}) and the fill factor (FF) as the SCR width increases. The short-circuit current density (J_{SC}) values increase with increasing SCR width and reach their maximum at a SCR value of 600 nm. As for the conversion efficiency, the values decrease for 100 nm≤ W_{SCR}≤200 nm then remain almost constant for 200 nm<W_{SCR}<600 nm. Beyond 600 nm, the conversion efficiency values gradually decrease. All the results show the need for an average SCR to obtain high performance and good stability (200≤W_{SCR}≤700 nm). Future research will consider the effects of donor and acceptor density in the performance optimization process.

Keywords

Solar PV Energy, Solar PV Cell, Space Charge Region, Internal Electric Field Strength, Numerical Simulation, Electrical Parameters

*Correspondence: Daouda Oubda (daoudaoubd@gmail.com)

Received: 17 August 2026; **Accepted:** 1 September 2026; **Published:** 20 September 2026

1. Introduction

In a global context marked by a constant increase in energy demand, the scarcity of fossil resources and growing environmental concerns, the search for alternative, clean and sustainable energy sources is becoming a necessity [1].

Several questions remain regarding the production of abundant, low-cost energy without environmental impact [2]. This is why the optimization of the performance of thin-film PV solar cells has been and continues to be the subject of several studies [3-7].

Regardless of the structure of a PV solar cell, optimizing its parameters is necessary to achieve good efficiency. Typically, the parameters to optimize are those whose variation is sensitive to the operation of the PV solar cell. The values of the optimal parameters depend, of course, on the solar cell structure, the quality of the material, the substrate (lifespan, mobility, diffusion length), the recombination velocity on the surface (front and back faces), and many other factors. Optimizing the performance of a PV solar cell therefore consists of studying the influence of these parameters on its overall behavior in order to obtain a structure that offers maximum efficiency.

The thin-film concept is very important. It should be noted that a variation on the order of a nanometer in the thickness of one of the layers: zinc oxide (ZnO) window layer, cadmium sulfured (CdS) buffer layer or Copper Indium Gallium diselenide.

($Cu(In,Ga)Se_2$) absorber layer in general, and in particular the width of the space charge region (W_{SCR}), has considerable effects on the operation of the PV solar cell. The W_{SCR} is the most sensitive and important part of the PV solar cell; it is where the majority of the photovoltaic solar process takes place. Optimizing the performance of the PV solar device must necessarily take into account the properties of the W_{SCR}. Figure 1 presents the model of the space charge zone, and equations (2) to (3) provide the expressions for the W_{SCR} width for a heterojunction and are used in the simulation.

In this article, our study focuses on numerically simulating the performance of our PV solar cell model. The aim of our study is to obtain improved electrical parameters. To achieve this objective, we opted for numerical simulation using SCAPS-1D software of the Mo/CIGS/CdS/ZnO structure.

2. Material and Method

2.1. Modeling of the SCR of the CIGS PV Solar Cell

When two semiconductors of different conductivities of type p and n are in contact with each other, a p-n junction is formed (Figure 1) and a space charge is created [8]. This is the origin of the appearance of a potential barrier and an internal electric field [8]. One of the most important characteristics of the p-n junction, which is taken into account in this article for the numerical simulation of the performance of our PV solar cell model, is the width of the space charge region (W_{SCR}) (Figure 1).

Figure 1 presents the space charge region model. Optimization consists of varying the parameter under study characterizing the PV solar cell (W_{SCR}) to reach maximum parameters. The structure of the solar cell studied is presented in our previous work [3, 7, 9].

We optimize the performance of the PV solar cell through the current-voltage density characteristic.

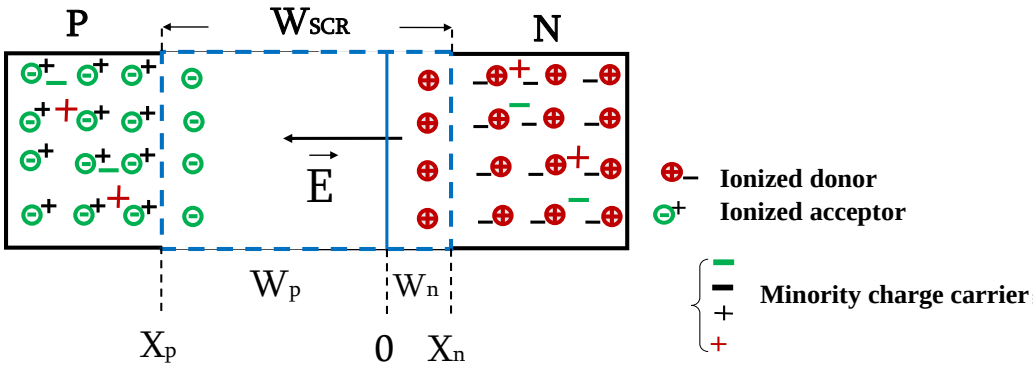

Figure 1. *Model of the space charge region of a p-n junction and the explanation of the constituants elements.*

Where Wp is the SCR created by positive charge carriers and Wn the SCR created by negative charge carriers. E, the internal electrostatic field.

In the case of a heterojunction, the SCR extends further into the p zone, a situation encountered in thin-film PV solar cells. Indeed, in the case of thin-film PV solar cells in general and in particular PV solar cells based on CIGS, the doping of the n-type layer is more important than that of the p-type layer. Consequently, most of the SCR is found in the p zone and allows better generation of charge carriers and obtaining better

conversion efficiency.

Using the continuity at the interface of the two semiconductors we have [10]:

$$N_D W_n = N_A W_p \quad (1)$$

The width of the SCR in darkness and without polarization is:

$$W = \sqrt{\frac{2\varepsilon}{q}\left(\frac{N_A + N_D}{N_A N_D}\right)V_{bi}} \quad (2)$$

Where V_{bi} is the internal potential

Under illumination and in open circuit:

$$W(V_{OC}) = \sqrt{\frac{2\varepsilon}{q}\left(\frac{N_A + N_D}{N_A N_D}\right)(V_{bi} - V_{OC})} \quad (3)$$

With N_D the density of donors in the semiconductor (n) and N_A the density of acceptors in the semiconductor (p).

When a solar PV cell is illuminated and feeds into an external circuit, its pn junction operates in a forward bias regime. Light energy (photons) creates electron-hole pairs in the semiconductor. The electric field in the depletion region separates these charges; electrons move toward the n-region and holes toward the p-region. The accumulation of charges creates an electromotive force that lowers the potential barrier of the junction. This charge accumulation reduces the height of the potential barrier, which in turn lowers the effect of the internal voltage, thus decreasing the width of the depletion region.

Finally, it should be noted that our study is based on the case of a highly asymmetric junction, which implies that:

$$N_d \gg N_a \ , \ W_n \ll W_p$$

And

$$W = W_p + W_n \approx W_p \quad (4)$$

We have:

$$W_p = \left(\frac{2\varepsilon}{qN_a}(V_d + V_i)\right)^{1/2} \quad (5)$$

2.2. Parameters in Numerical Simulation

We consider any metal-semiconductor contact to be ohmic, on the one hand thanks to the consideration of the formation of the molybdenum diselenide ($MoSe_2$) layer at the back contact/CIGS layer interface in accordance with Jonas Petterson [11] and on the other hand thanks to the choice of the work outputs of the metal layers (front and back contacts) for the simulation (Table 1).

The back contact layer (metallic) is made of molybdenum (Mo), it ensures the collection of positive charges which result from the conversion of incident photons into electron-hole pairs. The permeability of this layer allows sodium atoms to diffuse and contribute to the best growth of the absorber at low and high temperature [12-15].

Similarly, selenium and gallium from the absorber diffuse into the molybdenum and form molybdenum diselenide ($MoSe_2$) in very small quantities after annealing at 600 ℃ [16-18]. The good ohmic and electronic behavior of the Mo/CIGS interface is due to the formation of the thin $MoSe_2$ layer [15, 17, 19], which allows for better adhesion of the molybdenum layer to the glass. The role of the $MoSe_2$ layer, approximately 10 nm thick, has been discussed within the CIGS community [16, 18]. It is now established that $MoSe_2$ is essential for facilitating the formation of a quasi-ohmic electrical contact at the interface between CIGS and molybdenum [16]. $MoSe_2$ has a band gap of 1.41 eV, which reduces recombination at the Mo/CIGS interface [18, 19]. The main advantage of this layer is its high stability at high temperatures [16], which directly impacts sodium diffusion [15, 16]. The $MoSe_2$ layer also improves CIGS adhesion to the molybdenum layer [16, 17, 20] and allows for better open-circuit voltage [18].

Regarding reflection, we neglected the reflection at the rear contact in our simulation due to the significant thickness of the absorber (W_{CIGS} > 100 nm). However, we did consider the reflection at the front contact, since the incident light arrives at this face, resulting in substantial photon loss. This photon loss greatly impacts the performance of the PV solar cell, particularly the short-circuit current density. In many modeling tools, this reflection represents 10% of the incident photons [21, 22], we have fixed the front-face reflection to this value.

2.3. SCAPS − 1D Simulation Software

Several software programs have been developed to numerically simulate solar PV cell models. They offer different possibilities and limitations for PV, but the basic principle remains the same. Among these programs, Analysis for Microelectronic and Photonic Structures (AMPS−1D) and Solar Cell Capacitance Simulator (SCAPS−1D) stand out.

SCAPS-1D is a Windows application developed by Marc Burgelman's team in the Department of Electronics and Information Systems (ELIS) at Ghent University in Belgium. SCAPS-1D is a one-dimensional numerical simulation software. It was developed to obtain the electrical characteristics of heterojunction and thin-film solar PV cells. Its development is inspired by work on CdTe and $Cu(In,Ga)Se_2$-based solar PV cells [23, 24]. The simulated results were in very good agreement with measured results [25] and with results obtained using previously developed software such as AMPS-1D [26]. SCAPS-1D allows for the simulation of structures consisting of seven (7) intermediate layers in addition to the front and

back contacts for an arbitrary light spectrum, which is a particular advantage. All physical and electronic properties can be displayed and modified in a separate window. Simple models are used for temperature dependence, effective density of states, and thermal agitation velocity. Other parameters such as thickness, band gap, and charge carrier mobilities also come into play in the simulation and have been the subject of our previous publications [3, 5, 7, 9, 27, 28].

Once the desired simulation is complete, the energy band diagram, generation-recombination profile, and current-voltage, capacitance-voltage, capacitance-frequency, and quantum efficiency curves of the photovoltaic device are displayed on the screen. Numerical data for these parameters can also be extracted and analyzed. This functionality makes SCAPS a very attractive program and justifies our choice.

Table 1 below presents the electrical and optical parameters of the different layers involved in the numerical simulation with SCAPS−1D.

Table 1. *Base parameters of CIGS cell properties.* Φ_b *—barrier height, Se and* S_h*—surface recombination velocity electron and hole,* N_C *and* N_V *—effective density of states,* N_{AG} *—acceptor-like defect density,* N_{DG} *—donor-like defect density,* E_A *and* E_D *—peak energy in,* σ_e *and,* σ_h *—capture cross section electrons and holes,* υ *—thermal velocity,* W_G *—characteristic energy. [3, 4, 5, 7, 22, 28, 29, 30, 31].*

Parameters	CIGS	CdS	ZnO
W(nm)	1000	30	100
Eg(eV)	1,2	2,4	3,3
χe(eV)	4,5	4,45	4,45
$\varepsilon/\varepsilon_0$	13,6	10	9
N_C(cm^{-3})	$2,2x10^{18}$	$2,2x10^{18}$	$2,2x10^{18}$
N_V(cm^{-3})	$1,8x10^{19}$	$1,8x10^{19}$	$1,8x10^{19}$
υ_e(cm/s)	$5x10^6$	10^7	10^7
υ_h(cm/s)	$5x10^6$	10^7	10^7
μ_e(cm^2/Vs)	10^2	10^2	10^2
μ_h(cm^2/Vs)	25	25	25
N_A [cm^{-3}]	$1,5x10^{12}$	-	-
N_D [cm^{-3}]	-	$2,5x10^{16}$	10^{18}
σe [cm^2]	10^{-16}	10^{-12}	10^{-14}
σe [cm^2]	10^{-16}	10^{-12}	10^{-15}
Parameters	Right	Left	
Φ_b [eV]	Φ_{bn}=0,0	Φ_{bp}=0,15	
Se [cm/s]	10^7	10^7	
S_h [cm/s]	10^7	10^7	
Reflectivity	0,05	0,8	

3. Results and Discussions

3.1. Internal Electric Field

Figure 4 shows the evolution of the internal electric field as a function of the width of the space charge region (SCR). We observe that the intensity of the internal electric field decreases drastically with increasing space charge zone width and is in agreement with Equation (5). We also note that our results are in good agreement with data from the literature [31].

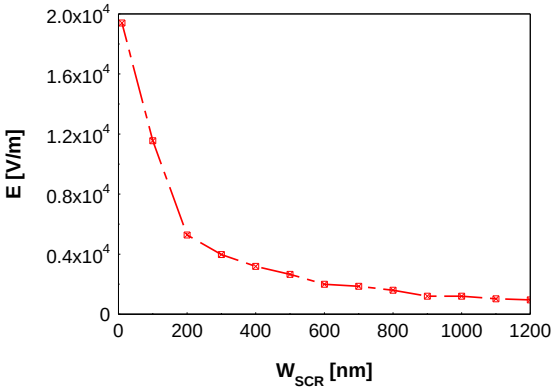

Figure 2. *Evolution of the internal electric field as a function of the SCR width.*

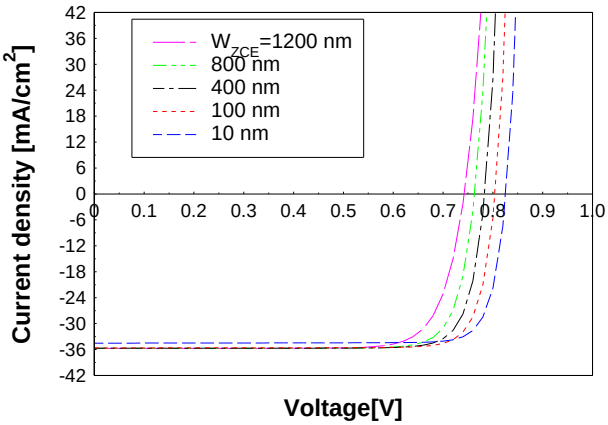

Figure 3. *J-V curves as a function of the width of the SCR.*

On the one hand, we note that the intensity of the electrical field is directly proportional to the potential difference (ΔV) and inversely proportional to the distance (d) as indicated by equation (6):

$$E = \Delta V / d \tag{6}$$

For our study, the distance "d" corresponds to the width of the SCR (W_{SCR}), which gives:

$$E = \Delta V / W_{ZCE} \tag{7}$$

For a very wide SCR, the electric field strength is very low. On the other hand, we have:

$$E_{\max} = \frac{qN_A W_p}{\varepsilon} = \frac{qN_D W_n}{\varepsilon} \tag{8}$$

The maximum intensity of the internal electric field (E_{int}) is proportional to the density of acceptors (N_A) or donors (N_D), therefore when the density of acceptors or donors doping decreases, the intensity of the E field decreases.

The decrease in the intensity of the electric field with the widening of the ZCE can result in an increase in the level of recombination phenomena, which can lead to a decrease in the performance of our solar PV device.

3.2. Current-voltage Density Characteristic

Figure 3 represents the J-V characteristic as a function of the width of the SCR.

We observe that as the width of the depletion region increases, the short-circuit current density increases despite a decrease in the electric field strength; however, the open-circuit voltage of the PV solar cell decreases (Figure 3).

These results can be explained by the increasing generation of electron-hole pairs in the SCR as its width increases.

3.3. Electrical Parameters

Regarding the electrical parameters, we note in addition to the V_{OC} (Figure 4), a significant decrease in the FF values with the increase in the width of the SCR (Figure 6).

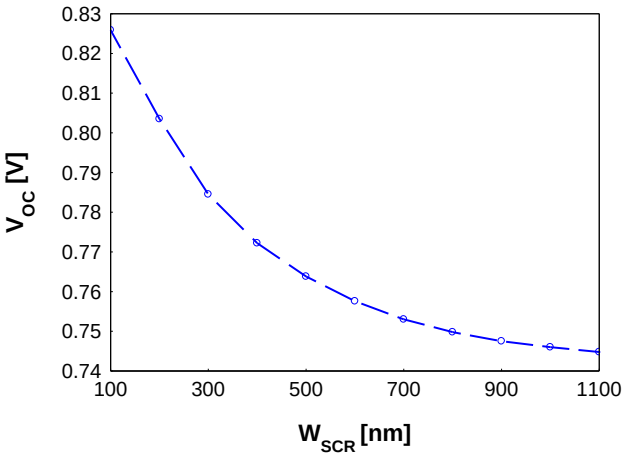

Figure 4. *V_{OC} as a function of SCR width.*

Indeed, the accumulation of electrons and holes creates an electric field and a voltage which oppose the initial internal electric field of the junction. As a result, the open circuit voltage Voc increases as the W_{SCR} decreases. [32-34].

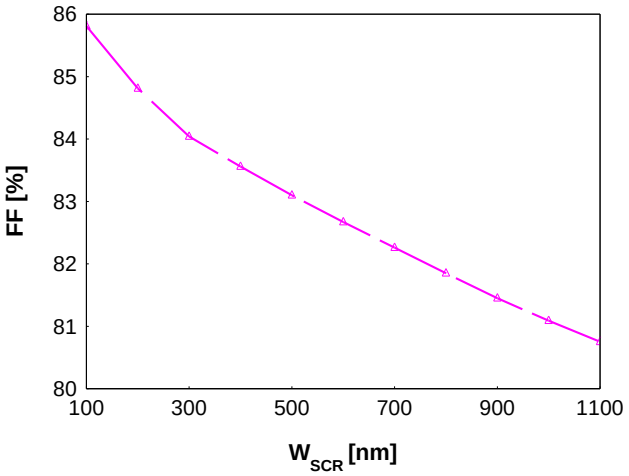

Figure 5. *FF as a function of SCR width.*

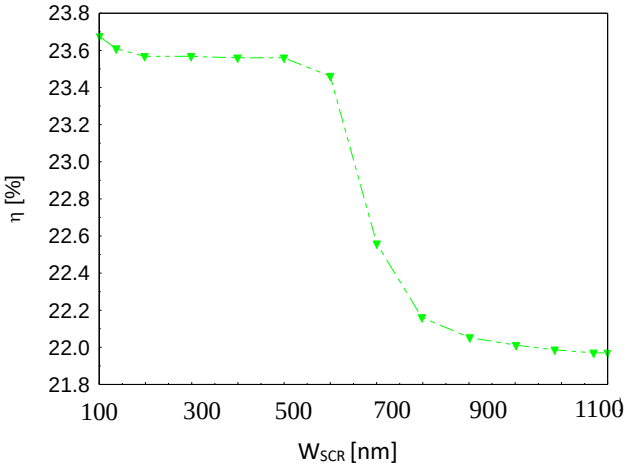

Figure 7. *Conversion efficiency as a function of SCR width.*

However, the short-circuit current density values (Figure 5) increase with increasing SCR width and reach their maximum at a W_{SCR} value of 600 nm. Beyond W_{SCR}=600 nm, the W_{SCR} values gradually decrease. As for the conversion efficiency (Figure 7), the values decrease for 100 nm≤W_{SCR}≤200 nm and then remain almost constant for 200 nm<W_{SCR}<600 nm. Beyond 600 nm, the conversion efficiency values gradually decrease.

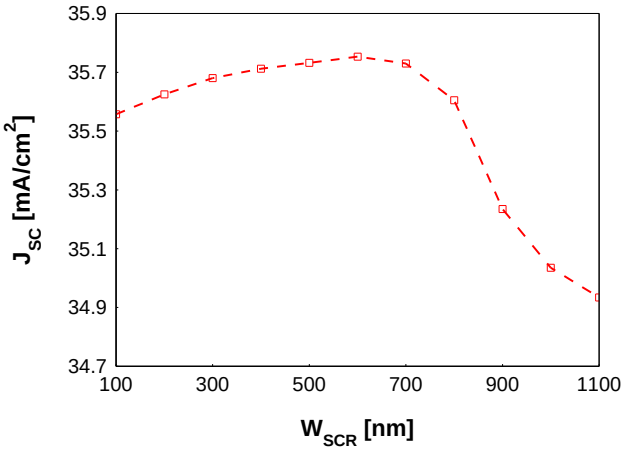

Figure 6. *J_{SC} as a function of SCR width.*

All of these results can be explained by the fact that, as the SCR width increases, the electric field strength decreases (Figure 2), leading to a corresponding increase in the recombination of photogenerated charge carriers. Furthermore, when the SCR width becomes very large due to a significant reduction in doping (Equation (2)) (SCR width >700 nm), the series resistance becomes substantial and can contribute to these results.

For optimal device performance at the maximum power point, an average SCR between 200 nm and 700 nm is required. A SCR between 200 and 700 nm facilitates significant electron-hole pair generation and also enables highly efficient separation and acceleration of these charge carriers due to the very strong electric field strength.

These results confirm the need for a relatively moderate SCR width for good performance of our CIGS-based solar PV cell model. Such a SCR width can be achieved by adjusting the doping of the solar PV device and the Ga concentration in the absorber.

Nima E. Gorji has indeed shown in these works that in the SCR, the absorption coefficient is assumed to be constant at a value of approximately 10^5 cm^{-1}. The choice of this constant value for the absorption coefficient in the SCR leads to a minimum depletion width of 400 nm, corresponding to an acceptor density of $2.75.10^{16}$ cm^{-3} [35].

4. Conclusion

In this article we present the role of the space charge region (SCR) in the performance optimization process of CIGS thin-film photovoltaic solar cells. The results of numerical simulations obtained with SCAPS-1D show that the SCR width plays a crucial role in this performance optimization process.

We also found that the maximum intensity of the internal electric field is proportional to the density of acceptors (N_A) or donors (N_D), therefore when the density of doping in acceptor or donor decreases, the maximum intensity of the electrical field decreases.

The decrease in the intensity of the electric field with the widening of the SCR would on the one hand be at the origin of the recombination phenomena responsible for the decrease in performance.

The results obtained show a significant decrease in V_{OC} and FF values with increasing SCR width. Short-circuit current density values increase with increasing SCR width and reach their maximum at a W_{SCR} value of 600 nm. Beyond W_{SCR}=600 nm, J_{SC} values gradually decrease. Conversion efficiency values decrease for 100 nm≤W_{SCR}≤200 nm, then remain almost constant for 200 nm< W_{SCR}<600 nm, and gradually decrease beyond 600 nm.

The various results demonstrate the need for a reduced SCR for high performance and good stability (200≤W_{SCR}≤700 nm). Future research will consider the effects of donor and acceptor density in the performance optimization process.

Abbreviations

AMPS−1D	Analysis for Microelectronic and Photonic Structures
CdS	Cadmium Sulfide
CdTe	Cadmium Telluride
CIGS	Copper Indium Gallium Selenide
Cu(In,Ga)Se_2	Copper Indium Gallium Diselenide
FF	Fill Factor
J_{SC}	Short Circuit Current Density
MO	Molybdenum
$MoSe_2$	Molybdenum Diselenide
PV	Photovoltaic
SCAPS-1D	One-dimensional Solar Cell Capacities Simulation
SCR	Space Charge Region
V_{bi}	Internal Potential
V_{OC}	Open Circuit Voltage
W_{SCR}	Space Charge Region Width
ZnO	Zinc Oxide

Author Contributions

Daouda Oubda: Conceptualization, Data curation, Formal Analysis, Funding acquisition, Investigation, Methodology, Software, Validation, Writing – original draft, Writing – review & editing

Alfred Bayala: Conceptualization, Data curation, Methodology, Project administration, Resources, Supervision, Validation, Writing – original draft, Writing – review & editing

Winde Nongue Daniel Koumbem: Conceptualization, Formal Analysis, Funding acquisition, Investigation, Methodology, Project administration, Resources, Software

Yacouba Coulibaly: Formal Analysis, Funding acquisition, Investigation, Methodology, Software, Supervision, Validation

Francois Zougmore: Conceptualization, Formal Analysis, Funding acquisition, Methodology, Project administration, Resources, Supervision, Validation, Visualization

Conflicts of Interest

The authors declare no conflicts of interest.

References

[1] Dupuis, J. 2009. Elaboration and characterization of SiO_xN_y: H and SiN_x: H layers produced by the PECVD method: application to the back side of silicon photovoltaic cells. Ph. D. thesis, Institute of Nanotechnologies of Lyon (INSA Lyon).

[2] Yan, X. 2014. Fabrication and characterization of $CuInGaSe_2$ films by sputtering. Study of defects by deep-trapping spectroscopy by charge. Ph. D. thesis, University of Nantes.

[3] Oubda, D., Kebre, M., Ouedraogo, S., Diasso, A., Zougmore, F., Koalga, Z., Ouattara, F. (2022) High Performance for Cu(In, Ga)Se_2 Quaternary System-Based Solar Cells with Alternative Buffer Layers. Advances in Materials Physics and Chemistry, 12, 207-209. https://doi.org/10.4236/ampc.2022.129015

[4] Ouedraogo, S., Kebre, M. B., Ngoupo, A. T., Oubda, D., Zougmore, F., Ndjaka, J.-M. (2020) Required CIGS and CIGS/Mo Interface Properties for High-Efficiency Cu(In, Ga)Se_2 Based Solar Cells. Advances in Materials Physics and Chemistry, 10, 151-166. https://doi.org/10.4236/ampc.2020.107011

[5] Zongo, A., Oubda, D., Ouedraogo, S., Kebre, M. B., Diasso, A., Sankara, I., Traore, B., Zougmore, F., Koalga, Z., Ouattara, F. (2021) Optimization of Mo/Cu(In,Ga)Se_2/CdS/ZnO Heterojunction Solar Cell Performance by Numerical Simulation with SCAPS-1D. Journal of Materials Science and Engineering B, 11, 156-167. https://doi.org/10.17265/2161-6221/2021.10-12.004

[6] Dullweber, T., Hanna, G., Shams-Kolahi., G., Schwartzlander, A., Contreras, M. A., Noufi, R., Schock, H. W. 2000. Study of the effect of gallium grading in Cu(In,Ga)Se_2. Thin Solid Films, 361-362, 478–481.

[7] Daouda, O., Marcel, B. K., Francois, Z., Donatien, N., Frederic, O. (2015) Numerical Simulation of Cu(In,Ga)Se_2 Solar Cells Performances. Journal of Energy and Power Engineering, 9, 1047-105. https://doi.org/10.17265/1934-8975/2015.12.002

[8] Oubda, D. (2018) Characterization of a Thin-Film Solar Cell Based on of CIGS Depending on the Nature of the Buffer Layer. University of Ouagadougou, Ouagadougou.

[9] Oubda, D., Kebre M. B., Ouedraogo, S., Zougmore, F., Ouattara, F., Koalga, Z. (2018) Numerical Characterization of Cu(In, Ga)Se_2 Solar Cells Using Capacitance-Voltage and Capacitance-Frequency Characteristics. International Journal of Progressive Sciences and Technologies, 6, 262-267.

[10] Souici, F. 2009, Modeling of a thin layer solar cell based on Copper Indium Selenium ($CuInSe_2$), magister. Kasdi Merbah Ouargla University.

[11] Pettersson, J. 2012. Modelling band gap gradiens and Cd-free buffer layers in Cu(In,Ga)Se_2 solar cells. Ph. D. thesis, Uppsalat University.

[12] Kessler, F., Dominik, R. 2004. Technological aspects of flexible CIGS solar cells and modules. Solar Energy, 77 (2004), 685695.

[13] Bena ïcha, M. 2010. Fabrication of ternary thin films by electrochemical means. Physic-chemical and electrical characterization. Ph. D. thesis, Ferhat Abbas University of S étif.

[14] Painchaud, T. 2010. Growth mechanisms of co-evaporated Cu(In,Ga)Se_2 thin films: towards rapid and low-temperature syntheses. Ph. D. thesis, University of Nantes.

[15] Buffiere, M., Harel, S., Arzel, L., Deudon, C., Barreau, N., Kessler, J. 2011. Fast chemical bath deposition of Zn(O,S) thin films for Cu(In,Ga)Se_2 solar cells. Thin Solid Films, 519, 575–7578.

[16] Abou-Ras, D., Kostorz, G., Bremaud, D., Kelin, M., Kurdesau, F. V., Tiwari, A. N., Debeli, M. 2005. Formation and characterisation of $MoSe_2$ for Cu(In,Ga)Se_2 based solar cells. Thin Solid Films 480481 (2005) 433 438, 480481 (2005), 433 438.

[17] Bollero, A., Kaupmees, L., Raadik, T., Grossberg, M., Fern ández, S. 2011. Thermal stability of sputtered Mo/polyimide films and formation of $MoSe_2$ and MoS_2 layers for application in flexible Cu(In,Ga)$(Se,S)_2$ based solar cells. Thin Solid Films, 2011, 6.

[18] Wei-Ting, L., Shih-Hao, C., Shao-Ze, T., Jhih-Jian, H., Sheng-Hui, C., Ruei-Fu, S., Chien-Wei, T., Tomi, T., L., Sung-Cheng, H., Wan-Xuan, P., Yung-Tien, L. 2014. Manipulation of $MoSe_2$ Films on CuIn(Ga)Se_2 Solar Cells during Rapid Thermal Process. Hindawi Publishing Corporation International Journal of Photoenergy, 2014, 5.

[19] Duchatelet, A. 2012. Synthesis of thin layers of Cu(In,Ga)Se_2 for solar cells by electrodeposition of mixed copper-indium-gallium oxides. Ph. D. thesis, Lille1 University.

[20] Ribeaucourt, L. 2011. Electrodeposition and selenization of Cu-In-Ga alloys for the synthesis of Cu(In,Ga)Se_2 thin films for solar cells. Ph. D. thesis, Universit é Pierre et Marie Curie.

[21] Gloeckler, M. 2005. Device physics of Cu(In,Ga)Se_2 thin-film solar cells. Ph. D. thesis, Colorado State University.

[22] Ouedraogo, S. 2016. Numerical modeling of a CIGS-based thin-film solar cell. Ph. D. thesis, University of Ouaga I Professor J. K. Zerbo.

[23] Niemegeers, A., Burgelman, M., Herberholz, R., Rau, U., Hariskos, D., Schock, H.-W. 1998. Model for electronic transport in Cu(In,Ga)Se_2 Solar Cells. Applied Physics Letters, 6, 407–421.

[24] Khelifi, S., Belghachi, A. 2004. The Role of the Window Layer in the Performance of a GaAs Solar Cell. Rev. Energ. Ren., Vol. 7 (2004), 13–21.

[25] Burgelman, M., Nollet, P., Degrave, S. 2000. Modelling polycrystalline semiconductor solar cells. Thin Solid Film, 361_362(2000); 527 -532:

[26] Yiming, L., Yun, S., Angus, R. 2011. A new simulation software of solar cells-wxAMPS. Solar Energy Materials and Solar Cells, (2011), https://doi.org/10.1016/j.solmat.2011.10.010 1–5.

[27] Oubda, D., Diasso, A., Ouedraogo, B., Kabre, S., Kebre, M. B., Ouedraogo, S., Traore, B., Zongo, A., Sankara, I., Sawadogo, P., Barry, A., Sawadogo, B. and Zougmore, F. (2025) Numerical Simulation of the Dominate Recombination Mechanism in the Chalcopyrite Cu(In,Ga)Se_2 Thin Film Solar Cell. Open Journal of Applied Sciences, 15, 3663-3672. https://doi.org/10.4236/ojapps.2025.1511238

[28] Oubda, D., Kabre S., Diasso A., Ouedraogo, B., Kebre M. B., Ouedraogo S., Traore B., Sankara I., Zongo, A., Barry A., Sawadogo B., Sawadogo P., Zougmore F. (2026) Simulation of the Effects of the Thickness and the Bandgap of the Absorber on the Performance of the Quaternary Thin Film Solar Cell Based on Cu(In,Ga)Se_2 Doctoral School of Sciences and Technologies, Joseph KI-ZERBO University, Ouagadougou, Burkina Faso. American Journal of Energy Engineering 2026, Vol. 14, No. 1, pp. 1–8 https://doi.org/10.11648/j.ajee.20261401.11

[29] Ouedraogo, S., Kebre, M. B., Ngoupo, A. T., Oubda, D., Zougmore, F. (2020) Comprehensive Analysis of $CuIn_{1-x}Ga_xSe_2$ Based Solar Cells with $Zn_{1-y}Mg_yO$ Buffer Layer. Materials Sciences and Applications, 11, 880-892. https://doi.org/10.4236/msa.2020.1112058

[30] Ouedraogo S., Traore B., Kebre B. M., Oubda D., Zongo A., Sankara I., Zougmore F. (2020). Performance Enhancement Strategy of Ultra-Thin CIGS Solar Cells. American Journal of Applied Sciences, 2020, Volume 17, pp. 246 255. https://doi.org/10.3844/ajassp.2020.246.255

[31] Shou-Yi K., Ming-Yang H., Dan-Hua H., Hao-Chung K., Chyong-Hua C., Fang-I L. (2014). Device Modeling of the Performance of Cu(In,Ga)Se_2 Solar Cells with V-Shaped Bandgap Profiles. https://doi.org/10.1155/2014/186579

[32] Pflieger J.-P., 2002. pn junction and diode. Marie and Louis Pasteur University. https://electronique.univ-fcomte

[33] No ël Servagent, 2004. Abrupt junction at thermodynamic equilibrium. Mens University, https://perso.univ-lemans.fr

[34] Abdelkrim Naas, 2020. the pn junction. Frere Mentouri University, https://telum.umc.edu.dz

[35] E. Gorji, U. Reggiani, L. Sandrolini. "A simple model for the photocurrent density of a graded band gap CIGS thin film solar cell", Solar Energy, vol. 86, no. 3, p. 920-925, March 2012. https://doi.org/10.1016/j.solener.2011.12.022